Few-Body Syst (2013) 54:57–62
DOI 10.1007/s00601-012-0329-y

**Y. Yamamoto · Th.A. Rijken**

# Realistic Effective *YN* Interactions in Hypernuclear Models

Received: 20 September 2011 / Accepted: 24 December 2011 / Published online: 13 March 2012


**Abstract** The features of the new interaction model ESC08 in $\Lambda N$, $\Sigma N$, $\Lambda\Lambda$ and $\Xi N$ channels are demonstrated on the basis of the G-matrix theory.

## 1 Introduction

One of fundamental problems in the strangeness nuclear physics is to reveal the entire picture of strong interactions among octet baryons. In studies of nuclear interactions, two-body scattering data are the primary input for setting interaction models. However, hyperon ($Y$)–nucleon ($N$) scattering data are very limited, and ambiguities of theoretical $YN$ interaction models are unavoidable. Then, effective $YN$ interactions used in hypernuclear models, adjusted so as to reproduce hypernuclear data, give valuable information on underlying interaction models.

Nice examples of our effective-interaction approach can be seen in analyses of light $\Lambda$ hypernuclei based on $\Lambda$-core(s) model. In 1990, the effective $\Lambda N$ interactions were derived from the available interaction models by the Nijmegen and Jeulich groups on the basis of the G-matrix theory, and applied to $\Lambda$-$^3$H($^3$He) folding model of ${}^4_\Lambda$H (${}^4_\Lambda$H) [1]. Then, the splitting energies of $0^+$–$1^+$ spin doublet states in these systems could not be reproduced reasonably by the adopted effective interactions, which means that their spin–spin interactions were inadequate. This analysis gave an important motivation to propose the new interaction model NSC97 [2], designed to give the reasonable spin–spin term.

## 2 G-Matrix Interaction

Properties of $\Lambda$, $\Sigma$ and $\Xi$ in nuclear medium are studied comprehensively on the basis of the G-matrix theory: We start from the channel-coupled G-matrix equation for the baryon pair ($\Lambda N$ and $\Sigma N$, etc.) in nuclear matter [3]. In G-matrix calculations, there are two ways to treat intermediate-state (off-shell) spectra: The simple one is the gap choice (GAP) which means that no potential term is taken into account. The other is the continuous choice (CON) where an off-shell potential is taken continuously from an on-shell potential. The nucleon rearrangement effect is taken into account in an averaged way by the factor $(1-\mathcal{K}_N)$, $\mathcal{K}_N$ being a nucleon correlation probability. When this effect is taken into account in the case of CON choice, the obtained G-matrices are denoted by CONr.

Y. Yamamoto (✉)
Institute for Physical and Chemical Research (RIKEN), Wako, Saitama, 351-0198, Japan
E-mail: ys_yamamoto@riken.jp

Th.A. Rijken
Astrophysics and Particle Physics, Radboud University, Nijmegen, The Netherlands

For various hypernuclear applications, it is convenient to construct $k_F$-dependent effective local potentials which simulate the G-matrices. Here we parameterize them in a three-range Gaussian form $\mathcal{G}_P^{ST}(r) = \sum_{i=1}^{3}(a_i + b_i k_F + c_i k_F^2)\exp(-r^2/\beta_i^2)$, whose parameters $(a_i, b_i, c_i)$ are determined so as to simulate the calculated G-matrix in each spin $(S)$, isospin $(T)$ and parity $(P)$ state. A hyperon-nucleus potential in a finite system is derived from $YN$ G-matrix interactions $\mathcal{G}_{P=\pm}^{ST}(r)$ by the expression

$$U_Y(\mathbf{r},\mathbf{r}') = \delta(\mathbf{r}-\mathbf{r}')\int d\mathbf{r}''\rho(\mathbf{r}'')\,V_{dr}(|\mathbf{r}-\mathbf{r}''|;k_F) + \rho(\mathbf{r},\mathbf{r}')V_{ex}(|\mathbf{r}-\mathbf{r}'|;k_F), \tag{1}$$

with $\begin{pmatrix} V_{dr} \\ V_{ex} \end{pmatrix} = \frac{1}{2(2t_Y+1)(2s_Y+1)}\sum_{TS}(2T+1)(2S+1)[\mathcal{G}_{\pm}^{ST} \pm \mathcal{G}_{\mp}^{ST}]$. Core nuclei are assumed to be spherical, and densities $\rho(r)$ and mixed densities $\rho(r,r')$ are obtained from Skyrme–Hartree–Fock (SkHF) wave functions. For $k_F$ values included in G-matrix interactions, we use the averaged-density approximation (ADA): An averaged value $\langle\rho\rangle$ is calculated by $\langle\phi_Y(r)|\rho(r)|\phi_Y(r)\rangle$ for each hyperon state $\phi_Y(r)$, $\langle k_F\rangle$ being obtained from $\langle\rho\rangle$. Then, a value of $\langle k_F\rangle$ is determined self-consistently for each hyperon state.

## 3 ESC08 Models

The new $YN \cdot YY$ interaction extended-soft-core model (ESC08) has been proposed by Rijken et al. [4], in which two-meson and meson-pair exchanges are taken into account explicitly. In the OBE models these effects are implicitly and roughly described by 'effective bosons'. There remain some serious problems in NSC97 and ESC04 models, ESC04 being the previous version of ESC08. The first is that the derived values of $\Lambda$ spin–orbit splitting energies are too large in comparison with the experimental values. The second is that the derived $\Sigma$-nucleus potentials $U_\Sigma$ are attractive, whereas the experimental values are indicated to be repulsive. The third is related to the $\Xi$-nucleus potentials $U_\Xi$, indicated to be rather attractive experimentally. The $U_\Xi$ values for NSC97 models are strongly repulsive. Those for ESC04a/b are weakly repulsive, and those for ESC04c/d are attractive though their partial-wave contributions seem to be rather problematic. These problems have been nicely solved in the ESC08 models, the treatments for axial-vector and pair terms are improved, and the effects of the quark Pauli-forbidden states in repulsive-core representations are taken into account. Especially, the latter effect is motivated by the success of the quark-cluster model of $YN \cdot YY$ interaction, and play decisive roles to reproduce repulsive (attractive) values of $U_\Sigma$ ($U_\Xi$) reasonably. Its essential part is that the Pauli-forbidden components exist in [51] states of the $SU(6)_{fs}$ representation.

In the older Nijmegen models including NSC97 and ESC04, repulsive cores are described dominantly by exchanges of pomerons and $\omega$ mesons. Then, the strengths of repulsive cores are similar with each other in all channels. In ESC08 modeling, pomeron–baryon coupling constants are strengthened phenomenologically in states including quark Pauli-forbidden components with large weights. In the cases of ESC08a/b, such effects are taken into account in $\Sigma^+p(^3S_1, T = 3/2)$, $\Sigma N(^1S_0, T = 1/2)$ and $\Xi N(^1S_0, T = 1)$ states, whose weights of [51] components are close to 1. In ESC08c, the pomeron–baryon coupling strength is taken faithfully to the weight value of [51] component in each state.

The quark Pauli-forbidden effects appear most clearly in potential energies $U_\Sigma$. In Table 1 we show the calculated values of $U_\Sigma(\rho_0)$ for a zero-momentum $\Sigma$ and their partial-wave contributions at normal density $\rho_0$, where a statistical factor $(2T+1)(2J+1)$ is included. It should be noted here that the repulsive values of $U_\Sigma$ can be obtained for ESC08a/b/c. In contrast, the $U_\Sigma$ values for ESC04a and NSC97f are attractive. In the cases of the repulsive values of $U_\Sigma$ for ESC08a/b/c, the most responsible is the contribution in $3S_1T = 3/2$ state, where the Pauli-forbidden state effect works strongly.

## 4 $\Lambda$ Hypernuclei

In Table 2 we show the potential energies $U_\Lambda$ for a zero-momentum $\Lambda$ and their partial-wave contributions $U_\Lambda(^{2S+1}L_J)$ at normal density $\rho_0$ ($k_F$=1.35 fm$^{-1}$) in the CONr case, where a statistical factor $(2J+1)$ is included in $U_\Lambda(^{2S+1}L_J)$. The obtained values for ESC08a/b/c are found to be very similar with each other. The values of $U_\Lambda = -(36-38)$ MeV seem to be too attractive compared to the experimental value of $-30$

**Table 1** Values of $U_\Sigma$ at normal density and partial wave contributions with GAP choice (in MeV)

| Model | $T$ | $^1S_0$ | $^3S_1$ | $^1P_1$ | $^3P_0$ | $^3P_1$ | $^3P_2$ | $D$ | $U_\Sigma$ |
|---|---|---|---|---|---|---|---|---|---|
| ESC08a | 1/2 | 11.4 | −23.4 | 1.7 | 1.9 | −5.0 | 0.0 | −0.7 | |
| | 3/2 | −12.2 | 44.1 | −4.1 | −2.3 | 5.1 | −3.9 | −0.2 | 12.2 |
| ESC08b | 1/2 | 10.4 | −25.4 | 1.4 | 2.5 | −5.9 | 0.3 | −0.8 | |
| | 3/2 | −11.0 | 52.2 | −3.0 | −2.8 | 5.6 | −4.8 | −0.1 | 18.5 |
| ESC08c | 1/2 | 11.1 | −17.7 | 2.4 | 1.8 | −5.9 | −1.0 | −0.7 | |
| | 3/2 | −12.5 | 33.7 | −5.9 | −2.0 | 5.6 | −2.1 | −0.3 | 6.3 |
| ESC04a | 1/2 | 11.6 | −26.9 | 2.4 | 2.7 | −6.4 | −2.0 | −0.8 | |
| | 3/2 | −11.3 | 2.6 | −6.8 | −2.3 | 5.9 | −5.1 | −0.2 | −36.5 |
| NSC97f | 1/2 | 14.9 | −8.3 | 2.1 | 2.5 | −4.6 | 0.5 | −0.5 | |
| | 3/2 | −12.4 | −4.1 | −4.1 | −2.1 | 6.0 | −2.8 | −0.1 | −12.9 |

**Table 2** Values of $U_\Lambda(\rho_0)$ and partial wave contributions with the CONr prescriptions (in MeV)

| Model | $^1S_0$ | $^3S_1$ | $^1P_1$ | $^3P_0$ | $^3P_1$ | $^3P_2$ | $D$ | $U_\Lambda$ | $U_{\sigma\sigma}$ |
|---|---|---|---|---|---|---|---|---|---|
| ESC08a | −12.5 | −24.1 | 2.4 | 0.0 | 1.2 | −3.3 | −1.5 | −37.8 | 1.12 |
| ESC08b | −12.1 | −22.4 | 2.1 | −0.2 | 1.3 | −3.8 | −1.6 | −36.7 | 1.17 |
| ESC08c | −12.9 | −23.1 | 2.6 | 0.1 | 1.2 | −2.9 | −1.5 | −36.4 | 1.29 |
| NSC97e | −11.9 | −26.1 | 1.7 | 0.4 | 2.6 | −1.2 | −1.1 | −35.8 | 0.81 |
| NSC97f | −13.2 | −23.5 | 2.0 | 0.3 | 3.3 | −0.8 | −1.2 | −33.1 | 1.36 |

Contributions from $S$-state spin–spin interactions are given by $U_{\sigma\sigma} = (U(^3S_1) - 3U(^1S_0))/12$

**Table 3** Strengths of $\Lambda$ spin–orbit splittings

| Model | $S_{SLS}$ | $S_{ALS}$ | $K_\Lambda$ |
|---|---|---|---|
| ESC08a | −20.6 | 16.5 | 4.3 |
| ESC08b | −21.8 | 16.5 | 5.5 |
| ESC08c | −19.7 | 14.8 | 5.1 |
| NSC97f | −19.7 | 7.2 | 13.1 |

See the text for the definitions of $K_\Lambda$ and $S_{SLS,ALS}$

MeV, which is the depth of the $\Lambda$ Woods–Saxon (WS) potential suitable to the data of $\Lambda$ hypernuclei. However, the WS depth strictly does not correspond to the $U_\Lambda$ value in normal-density nuclear matter. The $P$-state contributions for ESC08a/b (ESC08c) are slightly attractive (repulsive), which are constructive to the strongly repulsive contributions for NSC97e/f. The contributions to $U_\Lambda$ from $S$-state spin–spin components can be seen qualitatively in values of $U_{\sigma\sigma} = (U(^3S_1) - 3U(^1S_0))/12$. These values of $U_{\sigma\sigma}$ also are given in Table 2. Various analyses suggest that the reasonable value of $U_{\sigma\sigma}$ is between those of NSC97e and NSC97f, which are 0.81 and 1.36 MeV in the Table, respectively. Thus, the $S$-state spin–spin components of ESC08a/b/c turn out to be of reasonable strengths.

In order to compare clearly the $SLS$ and $ALS$ components, we derive the strengths of the $\Lambda l$-$s$ potentials in hypernuclei. With the Scheerbaum approximation [5], the expression is given as

$$U_\Lambda^{ls}(r) = K_\Lambda \frac{1}{r}\frac{d\rho}{dr}\mathbf{l}\cdot\mathbf{s} \quad \text{with} \quad K_\Lambda = -\frac{\pi}{3}(S_{SLS} + S_{ALS}), \tag{2}$$

where $S_{SLS,ALS} = \frac{3}{\bar{q}}\int_0^\infty r^3 dr\, j_1(\bar{q}r)\, \mathcal{G}_{SLS,ALS}(r)$ with $\bar{q} = 0.7$ fm$^{-1}$, and $\mathcal{G}_{SLS,ALS}$ are SLS and ALS G-matrix interactions, respectively. Table 3 shows the values of $K_\Lambda$ and $S_{SLS,ALS}$ calculated at $k_F = 1.0$ fm$^{-1}$ in the CONr case. The ALS parts in the ESC08a/b/c are more repulsive than that for NSC97f. The smaller values of $K_\Lambda$ in ESC08 cases are consistent with the experimental data.

Let us calculate $\Lambda$ s.p. energies in various $\Lambda$ hypernuclei with use of $\Lambda$-nucleus folding potentials from $\Lambda N$ G-matrix interactions. Here, we show results obtained by the G-matrix interaction for ESC08a (CONr). The energy spectrum of $^{89}_{\Lambda}$Y is of the most importance, since it has been observed in the $(\pi^+, K^+)$ reaction with an energy resolution of 1.65 MEV (FWHM) and in the highest statistics so far [6]. In this data, there appear clearly the double-peak structures in the observed energy spectrum. On the basis of elaborate shell-model analysis, it was shown that the observed energies of the left-side peaks were considered as the experimental values of $\Lambda$ s.p. energies in the ground-state core [7]. This experimental spectrum of $^{89}_{\Lambda}$Y can be reproduced

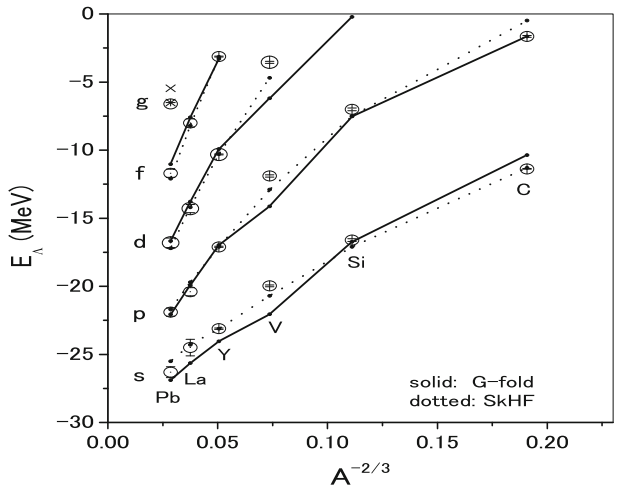


**Fig. 1** Energy spectra of ${}^{13}_{\Lambda}$C, ${}^{28}_{\Lambda}$Si, ${}^{51}_{\Lambda}$V, ${}^{89}_{\Lambda}$Y, ${}^{139}_{\Lambda}$La and ${}^{208}_{\Lambda}$Pb. *Solid* (*dashed*) *lines* show calculated values by the G-matrix folding model for ESC08a (the Skyrme–HF model). *Open circles* denote the experimental values

**Table 4** Calculated values of $B_{\Lambda\Lambda}$ (in MeV) with the $core + 2\Lambda$ models with $\Lambda\Lambda$ G-matrix interactions derived from ESC08a/b

| | ESC08a | ESC08b | EXP |
|---|---|---|---|
| ${}^{6}_{\Lambda\Lambda}$He | 7.1 (0.85) | 7.2 (0.86) | $6.91 \pm 0.16$ |
| ${}^{10}_{\Lambda\Lambda}$Be | 14.2 (1.01) | 14.5 (1.01) | $14.7 \pm 0.6$ |
| ${}^{11}_{\Lambda\Lambda}$Be | 18.7 (1.07) | 19.1 (1.07) | $20.83 \pm 1.27$ |
| ${}^{12}_{\Lambda\Lambda}$Be | 21.2 (1.11) | 21.6 (1.12) | $22.48 \pm 1.21$ |
| ${}^{13}_{\Lambda\Lambda}$B | 23.2 (1.16) | 23.6 (1.17) | $23.3 \pm 0.7$ |

Values in parentheses are $\langle k_F \rangle$ in fm$^{-1}$ obtained self-consistently

nicely by use of the G-matrix folding model derived from ESC08a (CONr) with almost no free parameter for fitting.

In Fig. 1, the energy spectra are shown for the observed $\Lambda$ hypernuclei (${}^{13}_{\Lambda}$C, ${}^{28}_{\Lambda}$Si, ${}^{51}_{\Lambda}$V, ${}^{89}_{\Lambda}$Y, ${}^{139}_{\Lambda}$La, ${}^{208}_{\Lambda}$Pb) [8] calculated with the G-matrix interactions for ESC08a(CONr). The calculated values shown by solid lines are compared with the experimental values [8] marked by open circles, where the horizontal axis is given as $A^{-2/3}$. Our G-matrix folding model turns out to reproduce the energy spectra of $\Lambda$ hypernuclei systematically almost with no free parameter. In Fig. 1, we show also the result (dashed lines) calculated by the SkHF model, where the $\Lambda N$ Skyrme parameters are determined only by using the observed spectrum of ${}^{89}_{\Lambda}$Y [4].

## 5 Double-$\Lambda$ Hypernuclei

We adopt here the model wave function is composed of two $\Lambda$ particles and a frozen-core nucleus. Coordinates of these $\Lambda$ particles are taken from the center-of-mass of the core. The core+$\Lambda\Lambda$ three-body state is represented as a superposition of Gaussian functions. Interactions are composed of $\Lambda$-core potentials and a $\Lambda\Lambda$ interaction. The $\Lambda$-core potential is chosen phenomenologically so as to reproduce the $\Lambda$-core binding energy. In this model space, high-momentum components of relative motions between two $\Lambda$'s are not included, and then $\Lambda\Lambda$ G-matrix interactions can be used safely without double counting.

The coupled-channel $G$-matrix equations in ${}^1S_0$ and ${}^3P_J T = 0$ states for $\Lambda\Lambda$, $\Xi N$ and $\Sigma\Sigma$ pairs in symmetric nuclear matter with the GAP choice. The obtained $\Lambda\Lambda G$-matrix interactions are represented by Gaussian functions in coordinate space. When this $\Lambda\Lambda$ G-matrix interaction $\mathcal{G}(r; k_F)$ is used in the present model, the $k_F$-dependent part is treated by ADA: The averaged value of $\langle k_F \rangle$ is defined as by the expectation value of averaged density by the core+$\Lambda\Lambda$ wave functions.

In Table 4, we show the calculated values of the three-body binding energy $B_{\Lambda\Lambda}$ in the cases of using the $\Lambda\Lambda$ G-matrix interactions derived from ESC08a/b, which are compared with the observed values in emulsion,

**Table 5** $U_\Xi(\rho_0)$ and partial wave contributions (in MeV)

| | $T$ | $^1S_0$ | $^3S_1$ | $^1P_1$ | $^3P_0$ | $^3P_1$ | $^3P_2$ | $U_\Xi$ | $\Gamma_\Xi$ |
|---|---|---|---|---|---|---|---|---|---|
| ESC08c | 0 | 3.6 | −8.3 | 0.2 | −4.9 | 2.0 | −0.8 | | |
| (CONr) | 1 | 12.0 | −12.3 | 2.2 | 1.3 | −1.6 | 1.7 | −4.4 | 4.6 |
| ESC08a | 0 | 6.1 | −0.9 | −0.3 | −2.8 | 1.4 | −1.0 | | |
| (GAP) | 1 | 21.8 | −31.7 | 2.5 | 0.3 | −3.7 | −0.6 | −9.0 | 7.6 |
| ESC08b | 0 | 2.1 | 2.0 | −0.6 | −1.3 | −0.1 | −0.7 | | |
| (GAP) | 1 | 26.6 | −40.3 | 3.0 | −0.6 | −3.7 | −1.3 | −14.7 | 2.7 |

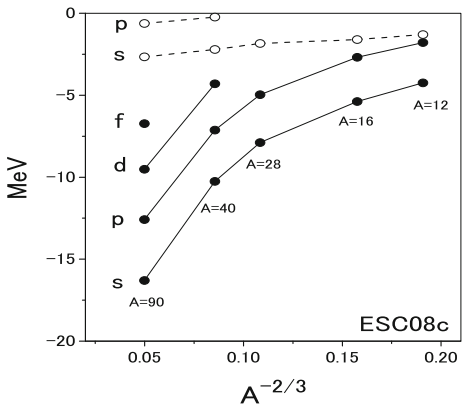


**Fig. 2** Energy levels of $\Xi^-$ hypernuclei calculated with the G-matrix folding model for ESC08c are shown by *full circles* connected by *solid lines*. *Open circles* are obtained without Coulomb interactions

where the values in parentheses are the values of $\langle k_F \rangle$ obtained self-consistently in ADA. The experimental data of double-$\Lambda$ nuclei summarized in Ref. [9] are cited in Table 4. The calculated results are found to be nicely consistent with the these experimental data. Thus, we can say that the $\Lambda\Lambda$ interactions in ESC08a/b are of reasonable strengths.

## 6 $\Xi$ Hypernuclei

The BNL-E885 experiment [10] suggests that a $\Xi^-$ s.p. potential in $^{11}_{\Xi^-}$Be is given by the attractive Woods–Saxon potential with the depth $\sim$ −14 MeV (called WS14). The $\Xi^-s$-state binding energy in this case is −2.2 MeV without the Coulomb interaction. In Table 5 we show the calculated values of $U_\Xi(\rho_0)$ and their partial-wave contributions. In order to compare G-matrix folding potentials with WS14, we calculate $s$-state binding energies in $\Xi^-$-$^{11}$C systems including Coulomb forces. The obtained values are −3.65 and −4.89 MeV, respectively, for the G-matrix folding potential derived ESC08c and WS14: They are found to be comparative. ESC08a/b lead to more attractive values. Hereafter, we study how $\Xi^-$ hypernuclear states are produced by the $\Xi^-$-nucleus potentials for ESC08c.

We perform calculations for systems composed of spin- and isospin-saturated nuclear cores attached by a $\Xi^-$ particle; $^{12}$C+$\Xi^-$,$^{16}$O+$\Xi^-$,$^{28}$Si+$\Xi^-$,$^{40}$Ca+$\Xi^-$,$^{90}$Zr+$\Xi^-$, where Coulomb interactions between $\Xi^-$ and nuclear cores are included. In Fig. 2, full circles connected by solid lines show the s.p. energies of $\Xi^-$-bound states calculated with G-matrix folding potentials derived from ESC08c. The horizontal axis is taken as a function of $A^{-2/3}$. Open circles connected by dashed lines are obtained without Coulomb interactions. It should be noted that the Coulomb contributions to $\Xi^-$ binding energies are substantial in large mass-number region.

In order to investigate the possibility of observing $\Xi^-$ hypernuclear state, we calculate $K^+$ spectra of $(K^-, K^+)$ reactions on some targets with use of our G-matrix folding models. Calculations are performed with the Green's function method in DWIA [11]. In Fig. 3, we show the obtained $K^+$ spectra for $^{12}$C and $^{28}$Si targets at forward-angle with an incident momentum 1.65 GeV/$c$. We can see clearly the peaks of $p$- and $d$-bound states, respectively, in the cases of $^{12}$C and $^{28}$Si targets. Here, the experimental resolution is assumed to be 2 MeV. Our G-matrix folding potentials include imaginary parts originated from the $\Xi N$–$\Lambda\Lambda$ coupling parts in the underlying interaction model (ESC08c).

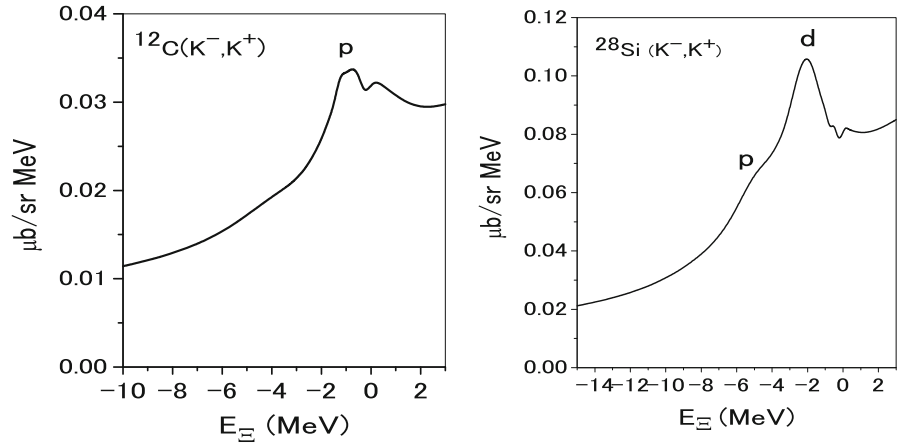


**Fig. 3** The spectra from ($K^-$, $K^+$) reactions on $^{12}$C (*left*) and $^{28}$ (*right*) targets

Thus, $\Xi^-$ hypernuclear states can be observed in ($K^-$, $K^+$) reactions even in the cases of shallow $\Xi$-nucleus potentials such as our G-matrix folding models derived from ESC08c.

## References

1. Yamamoto, Y., Motoba, T., Himeno, H., Ikeda, K., Nagata, S.: Hyperon–nucleon and hyperon–hyperon interactions in nuclei. Prog. Theor. Phys. Suppl. **117**, 361–389 (1994)
2. Rijken, Th.A., Stoks, V.G.J., Yamamoto, Y.: Soft-core hyperon–nucleon potentials. Phys. Rev. C **59**, 21–40 (1999)
3. Yamamoto, Y., Motoba, T., Rijken, Th.A.: G-matrix approach to hyperon–nucleus systems. Prog. Theor. Phys. Suppl. **185**, 72–105 (2010)
4. Rijken, Th.A., Nagels, M.N., Yamamoto, Y.: Baryon–baryon interactions. Prog. Theor. Phys. Suppl. **185**, 14–71 (2010)
5. Scheerbaum, R.R.: Spin–orbit splitting in nuclei near closed shells: (1). Contribution of the two-body spin–orbit interaction. Nucl. Phys. A **257**, 77–108 (1976)
6. Hotchi, H., et al.: Spectroscopy of medium-heavy $\Lambda$ hypernuclei via the ($\pi^+$, $K^+$) reaction. Phys. Rev. C **64**, 044302 (2001)
7. Motoba, T., Lanskoy, D.E., Millener, D.J., Yamamoto, Y.: $\Lambda$ spin–orbit splitting in heavy hypernuclei as deduced from DWIA analyses of the $^{89}$Y($\pi^+$, $K^+$)$^{89}_{\Lambda}$Y reaction. Nucl. Phys. A **804**, 99–115 (2008)
8. Hashimoto, O., Tamura, H.: Spectroscopy of $\Lambda$ hypernuclei. Prog. Part. Nucl. Phys. **57**, 564–653 (2006)
9. Nakazawa, K., Takahashi, H.: Experimental study of double-$\Lambda$ hypernuclei in nuclear emulsion. Prog. Theor. Phys. Suppl. **No.185**, 335–343 (2010)
10. Khaustov, P., et al.: Evidence of $\Xi$ hypernuclear production in the $^{12}$C($K^-$, $K^+$)$^{12}_{\Xi}$Be reaction. Phys. Rev. C **61**, 054603 (2000)
11. Tadokoro, S., Kobayashi, H., Akaishi, Y.: $\Xi^-$-hypernuclear states in heavy nuclei. Phys. Rev. C **51**, 2656–2663 (1995)